

2009

# Galaxies in a simulated Lambda CDM universe - II. Observable properties and constraints on feedback

D Keres

N Katz

*University of Massachusetts - Amherst, nsk@astro.umass.edu*

R Dave

M Fardal

DH Weinberg

Follow this and additional works at: [https://scholarworks.umass.edu/astro\\_faculty\\_pubs](https://scholarworks.umass.edu/astro_faculty_pubs)

 Part of the [Astrophysics and Astronomy Commons](#)

---

## Recommended Citation

Keres, D; Katz, N; Dave, R; Fardal, M; and Weinberg, DH, "Galaxies in a simulated Lambda CDM universe - II. Observable properties and constraints on feedback" (2009). *MONTHLY NOTICES OF THE ROYAL ASTRONOMICAL SOCIETY*. 303.

Retrieved from [https://scholarworks.umass.edu/astro\\_faculty\\_pubs/303](https://scholarworks.umass.edu/astro_faculty_pubs/303)

This Article is brought to you for free and open access by the Astronomy at ScholarWorks@UMass Amherst. It has been accepted for inclusion in Astronomy Department Faculty Publication Series by an authorized administrator of ScholarWorks@UMass Amherst. For more information, please contact [scholarworks@library.umass.edu](mailto:scholarworks@library.umass.edu).

# Galaxies in a Simulated $\Lambda$ CDM Universe II: Observable Properties and Constraints on Feedback

Dušan Kereš<sup>1</sup>, Neal Katz<sup>2</sup>, Romeel Davé<sup>3</sup>, Mark Fardal<sup>2</sup>, David H. Weinberg<sup>4</sup>

<sup>1</sup>*Institute for Theory and Computation, Harvard-Smithsonian Center for Astrophysics, Cambridge, MA 02138, dkere@cfh.harvard.edu*

<sup>2</sup>*Astronomy Department, University of Massachusetts at Amherst, MA 01003; nsk@astro.umass.edu, fardal@astro.umass.edu*

<sup>3</sup>*University of Arizona, Steward Observatory, Tucson, AZ 85721; rad@astro.as.arizona.edu*

<sup>4</sup>*Ohio State University, Department of Astronomy, Columbus, OH 43210; dhw@astronomy.ohio-state.edu*

5 May 2009

## ABSTRACT

We compare the properties of galaxies that form in a cosmological simulation without strong feedback to observations of the  $z = 0$  galaxy population. We confirm previous findings that models without strong feedback overproduce the observed galaxy baryonic mass function, especially at the low and high mass extremes. Through post-processing we investigate what kinds of feedback would be required to reproduce the statistics of observed galaxy masses and star formation rates. To mimic an extreme form of “preventive” feedback, such as a highly efficient AGN “radio mode,” we remove all baryonic mass that was originally accreted from shock-heated gas (“hot mode” accretion). This removal does not bring the high mass end of the galaxy mass function into agreement with observations because much of the stellar mass in these systems formed at high redshift from baryons that originally accreted via “cold mode” onto lower mass progenitors. An efficient “ejective” feedback mechanism, such as supernova-driven galactic winds, must reduce the masses of these progenitors before they merge to form today’s massive galaxies. Feedback must also reduce the masses of lower mass  $z = 0$  galaxies, which assemble at lower redshifts and have much lower star formation rates. If we monotonically remap galaxy masses to reproduce the observed mass function, but retain the simulation-predicted star formation rates, we obtain fairly good agreement with the observed sequence of star-forming galaxies. However, we fail to recover the observed population of passive, low star formation rate galaxies, especially at the high mass end. Suppressing all hot mode accretion improves the agreement for high mass galaxies, but it worsens the agreement at intermediate masses. Reproducing these  $z = 0$  observations requires a feedback mechanism that dramatically suppresses star formation in a *fraction* of galaxies, increasing with mass, while leaving star formation rates of other galaxies essentially unchanged.

**Key words:** cooling flows — feedback — cluster – galaxies: evolution — galaxies: formation — models: semi-analytic — models: numerical

## 1 INTRODUCTION

One of the oldest challenges in galaxy formation theory is to explain its overall inefficiency, specifically how to prevent too much gas from cooling onto the central galaxies of dark matter halos and forming stars, resulting in higher-mass galaxies at a given number density than observed (e.g. White & Frenk 1991). A second, related challenge is to explain the bimodality in galactic properties, where massive galaxies are typically red, elliptical and have very little star formation, while lower mass objects are blue, disk, star-forming galaxies (e.g. Kauffmann et al. 2003; Baldry et al.

2004). Early work on these problems emphasised the need for efficient feedback in low mass galaxies, to stop very early star formation and to be able to match the low mass end of the galaxy mass function (White & Frenk 1991). The mechanism most often invoked at the low-mass end is supernova-driven winds (Dekel & Silk 1986). These winds not only suppress galaxy masses in low-mass halos, but are also necessary to enrich the intergalactic medium with metals as observed. There has been substantial progress in understanding the basic scaling relations required for supernova-driven outflows: for example, the models most successful in explain-

ing the IGM metal distribution rely on scaling relations appropriate for momentum-driven winds (Murray et al. 2005; Oppenheimer & Davé 2006). However, it is not yet clear under which conditions these winds operate in general. If the feedback at low masses is a supernova-driven wind, it is more likely to be efficient at high redshifts, when galaxies had star formation rates that are an order of magnitude or more higher than they are today. At lower redshifts, efficient feedback is also needed in low mass objects, but winds are less likely to be sufficient to remove gas from galaxies (Mac Low & Ferrara 1999; Ferrara & Tolstoy 2000) owing to their lower star formation rates.

Much of the recent focus has been on the properties of massive galaxies. Some recent semi-analytic models (SAMs) of galaxy formation (e.g. Croton et al. 2006; Bower et al. 2006; Cattaneo et al. 2006; Somerville et al. 2008) are able to reproduce the global properties of massive ellipticals, which appeared too blue and too massive in earlier theoretical models. All these models suppress star formation in massive halos by means of feedback from Active Galactic Nuclei (AGN). In several models, supermassive black holes accreting gas that has cooled from the surrounding hot halo atmosphere provide strong feedback to the hot halo gas, which prevents or slows the gas cooling. This type of feedback from AGN is often called “radio mode” feedback, since it is believed to operate in massive radio galaxies. However, such feedback cannot directly change the galaxy morphology, which is believed to be changed by major mergers (Toomre 1977), i.e. mergers of galaxies with similar masses. During major mergers the rapid inflow of gas into the central parts can feed the black hole in the galactic centre, which in turn can ionise, heat, and expel the surrounding cold gas. In idealised simulations of such major mergers, this “quasar mode” feedback was also successful in preventing the accretion of gas after the merger (Di Matteo et al. 2005). However, these simulations are typically evolved outside of their cosmological environment and do not model the subsequent evolution of halos, so it is still unclear how long this “quasar mode” feedback effect lasts before gas can fall in from the intergalactic medium and once again start cooling onto the galaxy.

In our previous work (Kereš et al. 2005, K05, hereafter) and in the first paper in this series (Kereš et al. 2009, K09, hereafter), we followed the buildup of galaxies and halo gas in a  $\Lambda$ CDM universe (inflationary cold dark matter with a cosmological constant), using hydrodynamic simulations *without* any of the strong feedback processes just mentioned. We showed that it is the smooth accretion of intergalactic gas that dominates the global galactic gas supply, not accretion by merging, and that it proceeds via two stages. First, gas is accreted through filamentary streams, where it remains relatively cold before it reaches the galaxy (Katz et al. 2003, K05). This accretion mode, which we call cold mode accretion, is very efficient because the gas does not need to cool and hence it falls in on approximately a free-fall time. This means that the baryonic growth closely mimics the growth of the dark matter halo, albeit with a slight time delay. Cold mode accretion dominates the global growth of galaxies at high redshifts and the growth of lower mass objects at late times. As the dark matter halo grows larger, a larger fraction of the infalling material shock heats to temperatures close to the virial temperature. In the denser, cen-

tral regions a fraction of this hot gas is able to cool. This latter process is the “classical” scenario by which galaxies gain gas (e.g. Rees & Ostriker 1977; White & Rees 1978), and to differentiate it from the previous mode we call it hot mode accretion. The dominant accretion mode depends on halo mass, and the transition between these two regimes occurs at a mass of  $M_{\text{halo}} \sim 2\text{--}3 \times 10^{11} M_{\odot}$ . A similar (albeit slightly lower) transition mass between shock heated and non-shock heated halo gas is found in spherically symmetric calculations (Birnbom & Dekel 2003), and the physics behind this transition is apparently related to the ratio of post-shock compression and cooling times. In halos with masses near the transition mass, cold filamentary flows still supply the central galaxy with gas even though some of the infalling gas shock heats to near the virial temperature. At higher redshifts cold filaments are even able to survive within halos above this transition mass, i.e. halos dominated by hot halo gas (K05, Dekel & Birnbom 2006; Ocvirk et al. 2008, K09). Overall, the bulk of the baryonic mass in galaxies is accreted through the cold accretion mode and on average no galaxy of any mass acquires more than about 30% of its mass through hot mode accretion (K09).

We can sort the galaxy feedback processes discussed above into two classes: those that prevent gas from entering a galaxy in the first place, “preventive” feedback, and those that expel a fraction of the gas that does manage to enter the galaxy, “ejective” feedback. AGN radio mode heating and photoionisation are examples of preventive feedback, while winds driven by supernovae or AGN “quasar mode” are examples of ejective feedback. (The same feedback process could in principle be both ejective and preventive—for example if the energy released in a quasar-driven wind heats the surrounding halo gas and thereby prevents it from cooling.) The effectiveness of these two feedback types should vary depending on the dominant accretion mode in the halo hosting the galaxy. Because cold mode halos have very little halo gas outside of the cold dense filaments, it is doubtful whether ejective feedback can drastically affect the accretion of gas. However, ejective feedback could lower the masses of galaxies in these halos by expelling already accreted material. In this case, whether or not the winds escaped into the IGM would only be determined by energetics (assuming winds cannot destroy dense filamentary streams of gas), since the halos are mostly devoid of gas. Such winds, however, might be stopped by the quasi-spherical, hot halos that surround hot mode galaxies, making them ineffective. Conversely, preventive feedback like the “radio mode” of AGN is likely most effective in hot mode halos, where it can prevent the hot, dilute gas that is in quasi-static equilibrium from cooling (as discussed in K05). The exceptions may be at very low masses, where photoionisation and preheating could prevent gas from getting into the halos in the first place by strongly reducing the gas cooling rates.

To understand the role of feedback during galaxy formation and evolution, one also has to understand how galaxies are supplied with baryons and in particular with the gas that provides the fuel for star formation. This is difficult with current SAMs, as they do not yet accurately track cold mode accretion. On the other hand, simulations currently lack the resolution necessary to accurately simulate either preventive or ejective feedback processes directly within a cosmological environment. Therefore, it is important to gain

understanding of when and where feedback is necessary to explain the observed properties of galaxies. In this paper we do this from the vantage point of our own cosmological simulations, which do not include *any* strong feedback mechanisms. By comparing the observed properties of galaxies with the galaxies that form in our simulations, we confirm the conventional wisdom that one or more strong feedback mechanisms are needed to prevent the excessive accumulation of baryons into galaxies. We draw inferences about where in redshift and galaxy/halo mass gas accretion must be suppressed and what feedback mechanisms are likely to be successful. To mimic an extreme version of preventive feedback, e.g., a perfectly efficient AGN “radio mode”, we remove all the gas accreted through hot mode from all galaxies. We show that this extreme feedback scenario only slightly improves the match between simulated and observed galaxy masses, which still disagree at the faint and bright ends<sup>1</sup>. Therefore ejective feedback from starburst winds is required. In addition, a selective feedback mechanism, like one that occurs primarily during major mergers, is probably required to explain the bimodality of the galaxy population.

A large fraction of the results presented in this paper are presented in slightly different form as a part of D. Kereš’s PhD thesis at University of Massachusetts, Amherst (Keres 2007).

In §2 we describe our new simulations, and the specifics of our procedure for removing hot mode accretion, as well as the “cold drizzle” in massive galaxies which we suspect to be numerically enhanced. In §3.1 we compare the observed stellar mass function of galaxies to that of simulated galaxies both with and without hot mode accretion. We discuss in §3.2 the accumulation of galaxy mass and the stellar component, and in §3.3 we compare the observed star formation rates with the simulations, again with and without hot mode accretion. We discuss the feedback mechanisms needed to bring the masses and specific star formation rates of the simulated galaxies into better agreement with the observations in §4 and conclude in §5.

## 2 SIMULATION

We described the simulation analysed in this paper in K09, but for completeness we summarise its main properties here. We adopt a cold dark matter model dominated by a cosmological constant,  $\Lambda$ CDM, with the following cosmological parameters:  $\Omega_m = 0.26$ ,  $\Omega_\Lambda = 0.74$ ,  $h \equiv H_0/(100 \text{ km s}^{-1} \text{ Mpc}^{-1}) = 0.71$ , and a primordial power spectrum index of  $n = 1.0$ . For the amplitude of the mass fluctuations we use  $\sigma_8 = 0.75$ , and for the baryonic density we adopt  $\Omega_b = 0.044$ . All of these cosmological parameters are consistent with the the newest measurements from the WMAP team (Spergel et al. 2007) and with vari-

<sup>1</sup> This conclusion is contrary to the conjecture of K05, most likely because the more accurate SPH formulation used here leads to much lower hot accretion rates (K09). The galaxy population in our present simulations is a better match to observations than that of K05, but suppression of hot mode produces little further improvement.

ous large scale structure measurements<sup>2</sup>, except for the primordial power spectrum index which is slightly higher in our simulations. We model a  $50.0h^{-1}$  Mpc comoving periodic cube using  $288^3$  dark matter and  $288^3$  gas particles, i.e. around 50 million particles in total. Gravitational forces are softened using a cubic spline kernel of comoving radius  $10h^{-1}$  kpc, approximately equivalent to a Plummer force softening of  $\epsilon_{\text{grav}} = 7.2h^{-1}$  kpc. Using the naming scheme from K09, we will refer to this simulation as L50/288 later throughout the text.

We include the relevant cooling processes using primordial abundances as in Katz et al. (1996), omitting cooling processes associated with heavy elements or molecular hydrogen. In all of these simulations we include a spatially uniform, extragalactic UV background that heats and ionises the gas. The background redshift distribution and spectrum are slightly different than in K05. The background flux starts at  $z = 9$  and is based on Haardt & Madau (2001). For more details about the calculation of this UV background see Oppenheimer & Davé (2006). We note here that smaller volume simulations with our new UV background and with the version used in K05 showed no noticeable differences in the evolution of the galaxy population in the redshift range  $0 < z < 4$  of interest in this paper.

The initial conditions are evolved using the SPH code Gadget-2 (Springel 2005). The calculation of the gravitational force is a combination of the Particle Mesh algorithm (Hockney & Eastwood 1981) for large distances and the hierarchical tree algorithm (Barnes & Hut 1986; Hernquist 1987) for small distances. The smoothed particle hydrodynamics algorithm (Lucy 1977; Gingold & Monaghan 1977) used here is entropy and energy conserving, and it is based on the version used in Springel & Hernquist (2002). The public version of this code was modified (both by V. Springel and by us) to include the cooling, the uniform UV background, and the two-phase star formation algorithm.

Once the particle reaches a density above the star forming threshold, star formation proceeds in a two-phase medium where the supernova energy released by type II SNe during star formation balances cold cloud formation and evaporation by the hot medium as in McKee & Ostriker (1977). This enables more stable gas rich disks, but it does not produce galactic outflows, i.e. SN feedback only provides disk pressurisation. In this model, the dependence of the star formation rate on density is still governed by a Schmidt law (Schmidt 1959). The model parameters are the same as in Springel & Hernquist (2003), which were selected to match the  $z = 0$  Kennicutt law (Kennicutt 1998). The threshold density for star formation is the density where the mass-weighted temperature of the two phase medium equals 10,000 K. In practice, this threshold density remains constant in physical units during the simulation and corresponds to a hydrogen number density of  $n_h = 0.13 \text{ cm}^{-3}$ . Each gas particle within the two-phase medium has an assigned star formation rate but the actual conversion from gas to star particles occurs stochastically (Springel & Hernquist 2003), similar to the algorithm in Katz (1992). Each star

<sup>2</sup> <http://lambda.gsfc.nasa.gov/product/map/dr2/parameters.cfm> (see the  $\Lambda$ CDM/All values)

particle inherits half of the initial gas mass of the gas particle.

To identify bound groups of cold, dense baryonic particles and stars, which represent galaxies, we use the program SKID<sup>3</sup> (see K05 for more details). Briefly, a galaxy identified by SKID contains gravitationally bound groups of stars and gas with an overdensity higher than 1000 relative to the mean baryonic density and  $T < 3 \times 10^4$  K. Here, we slightly alter these criteria by using an increased temperature criterion at densities where the two-phase medium develops to allow star-forming, two-phase medium particles to be part of a SKID group, since at high densities the mass-weighted temperatures in the two phase medium can be higher than  $10^5$  K. After the identification of a galaxy (SKID group), we determine its total stellar mass and star formation rate. The stellar mass is simply the sum of the masses of the star particles and the “instantaneous” star formation rate is the sum of the “instantaneous” star formation rates of all the gas particles, calculated from the properties of the two-phase medium.

The simulation here accounts for mass loss from stars that explode as Type II supernovae, but not for the larger fraction of mass lost from intermediate-mass stars, which can be 0.3–0.4 at late times for a Kroupa (2001) or Kroupa & de Jong (2001) IMF (Bell & de Jong 2001). After beginning the simulation discussed in this paper, we added this effect to the code and tested it in smaller volume simulations. We find very similar rates of stellar mass lockup in the two simulations. In other words, the global density of stars as a function of redshift remains nearly unchanged, but the global star formation rates increase, by up to factor 2 at late times. Thus, we expect delayed recycling to have little effect on the masses or stellar ages of a typical galaxy but to boost the individual star formation rates by about a factor 2. We caution, however, that this test was performed using simulations without strong feedback. Ejective feedback processes might succeed in removing the recycled gas before it forms stars, thus resulting in lowered stellar masses and smaller increases in the star formation rate. We will comment in more detail on the possible effects of mass feedback in §3.3.

### 2.1 Removing hot mode accretion

In K05, we showed that much of the gas in galaxies entered through cold mode, and we argued that removing a large fraction of the remaining hot mode accretion could bring the simulated galaxies into better agreement with the observed galaxy masses and colours. The simulation method used in K05 in fact suffered from numerically enhanced hot-mode cooling rates (Pearce et al. 2001; Springel & Hernquist 2002), owing to an enhanced density of the hot phase at hot-cold boundaries. Our new simulation has a much larger volume and contains many more galaxies in massive halos, and it also uses an SPH algorithm that prevents numerical overcooling. Thus we can more reliably test the significance of hot mode accretion.

Models of preventive feedback suppress the hot mode

accretion to varying degrees. For example, in models of “radio mode” feedback (Croton et al. 2006), a black hole at the centre of its halo suppresses the accretion only if it contains enough mass to provide a significant input of energy into the halo gas and only if it resides in a halo containing a significant hot atmosphere, and it need not be 100 percent effective. However, the SAM of Cattaneo et al. (2006) assumes the complete shut-down of accretion in massive halos, above a critical mass and below a critical redshift. In our case, to mimic the most extreme case of preventive feedback, we choose to completely ignore *all* the gas particles that cool from any hot halo, regardless of halo mass or redshift.

The method we use to identify hot mode accretion is similar to that used in K05. Starting with particles in galaxies at  $z = 0$ , we follow the particles back through time and flag all the particles that have ever reached a temperature higher than  $2.5 \times 10^5$  K. (Particles within the star-forming two-phase medium can exceed this threshold owing to the contribution from the hot phase to the mass-weighted temperature. Here we ignore these particles, since they clearly have already been accreted into a galaxy.) Then we produce a new, revised list of galaxy stellar, gas, and total masses along with galactic star formation rates, excluding the contribution from particles flagged as accreting through hot mode.

### 2.2 Removing cold mode accretion in massive galaxies

In K09, we showed that in Gadget-2 simulations massive halos contain many cold clumps of gas that are not identified by SKID as galaxies. Such clumps survive within the hot halo gas, and because the ram pressure drag on such objects is likely overestimated, they fall onto the central galaxy in just over a free-fall time, a process we term “cold drizzle”. As a result, the contribution of cold mode to the total gas accretion falls to a minimum around a galaxy mass of  $10^{11} M_{\odot}$  and then rises again at higher masses (see Figure 8 of K09). Whether or not such cold clumps should form and survive in very hot halos is not clear (see the discussion in K09). However, the accretion rate of these clumps is almost certainly overestimated, since in most SPH implementations the effective cross-section for ram pressure is overestimated at low resolution, increasing the drag on a cold clump as it moves through a hot medium (Tittley et al. 2001). Furthermore, it is possible that many of these clumps would be destroyed by surface instabilities that are hard to model correctly in SPH (Agertz et al. 2007) or by conduction.

To bracket the correct solution, therefore, we remove cold mode accretion onto galaxies more massive than  $10^{11} M_{\odot}$  to see how the properties of our simulated galaxies change. We use the galaxy’s mass at the time the gas particle accretes (without adjusting its mass for hot mode removal). Even though this cutoff mass is well into the hot mode regime, a large mass fraction of these massive galaxies is built up by gas initially accreted through cold mode, if it joined the massive galaxy through mergers. We do not remove this indirect cold mode accretion but since some of the sub-resolution SKID identified groups are also cold clouds, we also remove all the gas that was accreted from progenitors below our resolution limit of 64 particles to make the

<sup>3</sup> <http://www-hpcc.astro.washington.edu/tools/skid.html>

effect of cloud removal more extreme. We then recalculate the galaxy properties.

### 3 RESULTS

#### 3.1 The Stellar Mass Function

We begin the comparison of simulated and observed galaxy properties with the  $z \sim 0$  stellar mass functions (SMF). In Figure 1 we compare the observed ( $g$ -band derived) SMF from Bell et al. (2003) to the SMF from our L50/288 simulation. We plot the SMF starting from our adopted resolution limit. The stellar masses in Bell et al. (2003) are based on data from the SDDS survey (York et al. 2000) and the diet Salpeter IMF, and are shown to be consistent with the masses derived from the near infrared 2MASS survey (Skrutskie et al. 2006). The simulated galaxies are over-abundant at all galaxy masses, with the largest disagreements occurring at the low and high mass ends. By matching the integrated number density of galaxies above a certain mass in the simulation with the observations, we estimate the difference in mass between the observed and simulated galaxies (assuming the same rank ordering of galaxies by mass in the simulation and observations). We show this difference as a correction factor  $f_{\text{corr}} = M_{\text{sim}}/M_{\text{match}}$  in the lower panel of Figure 1.

The masses of the most massive simulated galaxies are about a factor of 3–5 higher than those observed. One can immediately conclude that strong feedback, which is not included in our simulations, is needed to decrease the masses of these simulated massive galaxies. The differences decrease at intermediate masses, around the “knee” of the observed mass function, where the simulated masses are only high by a factor of 1.5–2. At masses lower than several times  $10^{10} M_{\odot}$  the differences between the observed and simulated stellar mass function are enormous. To match the number density of observed galaxies requires suppressing the masses of the simulated galaxies by more than an order of magnitude. These differences suggest that a very efficient mechanism must prevent the formation of the majority of low mass galaxies with masses up to several times  $10^{10} M_{\odot}$  or that it must drastically lower their masses to bring the simulated galaxies into agreement with the observations.<sup>4</sup> Another possibility is that the observed galaxies contain significantly more gas and less stars at similar galaxy masses. Of course these conclusion are not new or unique to our work, and we will discuss the required properties of this mechanism in more detail in the discussion section. The total amount of baryons locked in the stellar component in our simulation is 18 percent, which is about a factor of 3 higher than the observed value (e.g. Bell et al. 2003). While the differences

<sup>4</sup> At the low mass end, the simulated galaxy SMF turns over and stays quite shallow, similar in slope to the observed mass function. We believe this to be a numerical artifact, since a higher-resolution simulation (see K09) shows no such feature. Apparently the UV background has an excessive effect on poorly resolved halos (Weinberg et al. 1997), slightly reducing the amount of baryons that can condense in halos even a factor of 2–3 higher than our adopted resolution limit. We will more fully investigate this effect and the quantitative influence of the UV background in future work.

between the simulated and observed galaxies are large at the high and low mass ends, the stellar masses of galaxies are in relatively good agreement around the “knee” of the mass function where a large fraction of the global stellar mass is concentrated, making this disagreement more moderate globally.

The galaxy masses in Figure 1 do not account for stars dispersed into the intracluster medium from the hierarchically built remnants. Observationally, in clusters of  $M_{\text{h}} \sim 3 \times 10^{14} M_{\odot}$ , about 20–30% of all stars in a halo are part of the ICM+central galaxy system, which is dominated by intracluster stars (ICS) (e.g. Gonzalez et al. 2007). In fractional terms this is not far from what we find in our simulated massive halos, which have 20–35% of their stars in the ICS at halo masses of about  $10^{14} M_{\odot}$ . The fraction of ICS stars is also subject to the exact definition of where the light of the central (brightest) cluster galaxy ends and becomes ICS and, therefore, any comparison of this aspect of our simulation to the observations is quite uncertain. However, the *combined* mass of the central galaxy and the ICS is already higher in our simulations than what is observed. Furthermore, most of the massive galaxies in our simulation are in halos of even lower mass, where ICS is likely an even less important stellar component. Given these facts, it appears unlikely that a large fraction of the factor of  $\sim 3$  larger galaxy mass in the simulations could be explained by having more ICS in the simulation.

In §2.1 we discussed removing the hot mode to mimic the extreme case of preventive feedback. We plot the SMF with hot mode accretion removed in Figure 1 (dashed line). We see that the decrease in galaxy masses caused by this extreme feedback does bring the simulations into better agreement with the observations at high masses, but the change in mass is only modest. The change is largest at intermediate masses, around the “knee” in the observed mass function. The typical change is several tens of percent at masses of around  $10^{11} M_{\odot}$  and is even smaller at higher masses. The removal of hot mode accretion even changes galaxy masses in objects with masses as small as several times  $10^{10} M_{\odot}$ , because there are still some galaxies at these small masses with significant hot mode accretion at low redshifts. At even lower masses, however, there is almost no change in mass after hot mode removal, which is not unexpected since all low mass galaxies are built exclusively through cold mode accretion.

The most surprising feature of this curve is the almost negligible change at the high-mass end. We conclude from this plot that the removal of hot mode accretion, to mimic an extreme case of preventive feedback such as an AGN radio mode, *cannot* explain the observed steep drop in the SMF at the high mass end. The removal of hot mode accretion only partially succeeds at intermediate masses, where the simulated mass function is indeed quite close to the observed one, but only over a small range of masses. Previously, in K09, we saw that the accretion of many galaxies at low redshift is completely dominated by hot mode accretion and yet their masses are not greatly affected by hot mode removal. We provide an explanation for this seeming contradiction in the next section and later, where we discuss the processes needed to bring the simulated galaxy masses into better agreement with the observations.

In §2.2 we discussed the removal of the cold gas infall

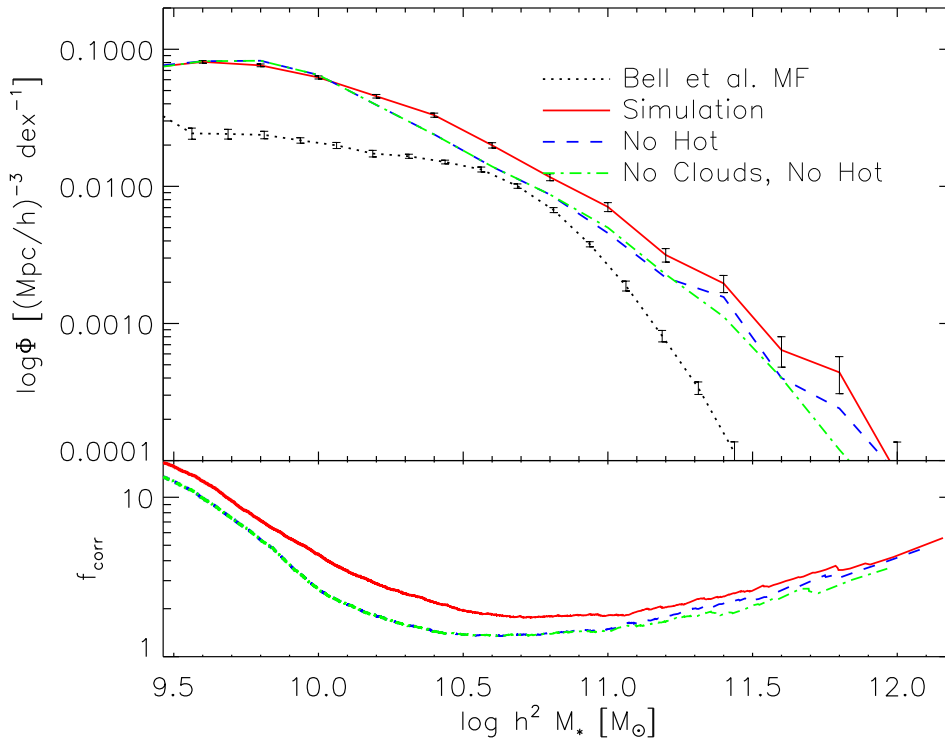


**Figure 1.** Upper panel: The observed stellar mass function of  $z \sim 0$  galaxies from Bell et al. (2003) (dotted) and the simulated stellar mass function (solid) at  $z = 0$ . We also plot the simulated stellar mass function when hot mode accretion is removed (dashed), to mimic extreme preventive feedback, and the mass function when both the hot mode and the potentially spurious cold-mode accretion in massive galaxies are removed (dot-dashed). The error bars indicate Poisson fluctuations in a given mass bin. Lower panel: The correction factor needed for simulated galaxies to match the observed galaxy masses at the same number density as a function of simulated stellar mass (see text for details).

in massive galaxies in addition to removing all hot mode, since we suspect this infall to be a numerical artifact. We show the results of this in Figure 1 as the dot-dashed line. The effect on massive galaxies is again rather small and, by construction, it only affects the most massive objects. Typically, most galaxies of around  $10^{12} M_{\odot}$  have their masses lowered by only  $\sim 20$  percent when the cold drizzle is removed. Therefore, even without cold mode accretion in massive galaxies, preventive feedback alone (such as an extreme AGN radio mode) is not sufficient to bring the high mass end of the observed and simulated SMFs into agreement.

### 3.2 Galaxy buildup and the fossil record

In Figure 2 (left), we plot lines showing the median redshift at which galaxies formed 25, 50, and 75 percent of their  $z = 0$  stellar mass as a function of the stellar mass of the galaxies. To indicate the scatter from one galaxy to another, we also show the mass weighted stellar formation redshift (the redshift when 50 percent of the  $z = 0$  stellar mass was formed) for each individual galaxy. The rising trend with mass has been described as the “downsizing” of galaxy formation. Sometimes this trend has been explained as a consequence of particular feedback models, but here we see that it is present in our SPH simulations *without* strong feedback, and therefore is a natural consequence of hierarchical models of galaxy formation (see also Dave 2006). Even the build-up of dark matter halos proceeds in a similar way,

where the bulk of the present halo mass of massive halos was already assembled in lower mass progenitors (above a given minimum mass) at earlier times than the bulk of the mass in low mass halos (Neistein et al. 2006).

For comparison, we also present in Figure 2 (right) observational estimates of the stellar formation redshifts from the spectral analysis galaxies from the Sloan Digital Sky Survey by Panter et al. (2007) (triangles). To generate these lines, we have taken the SFR as a function of redshift in each of five mass bins from their Figure 4, assumed the SFR to be constant within each redshift bin, extended the minimum redshift to  $z = 0$ , and interpolated the cumulative stars formed to get the 25 percent, 50 percent, and 75 percent redshifts. The analysis of Panter et al. (2007), made purely from the integrated spectra of the local galaxy population, is clearly difficult and subject to systematic errors (from the dust model, surface brightness biases, spectroscopic fibre coverage, or imperfections in the spectral modelling among others). The errors increase rapidly with the redshift, so the 25 percent curve is more reliable than the 75 percent one. However, the global behaviour of star formation and stellar mass as a function of redshift is in reasonable agreement with direct observations, and the overall “downsizing” picture inferred from this dataset has been confirmed by many previous studies. We also show the observationally inferred mass weighted stellar age from Gallazzi et al. (2008). Their analysis differs in detail from Panter et al. (2007), and it results in significantly younger stellar ages at all masses,

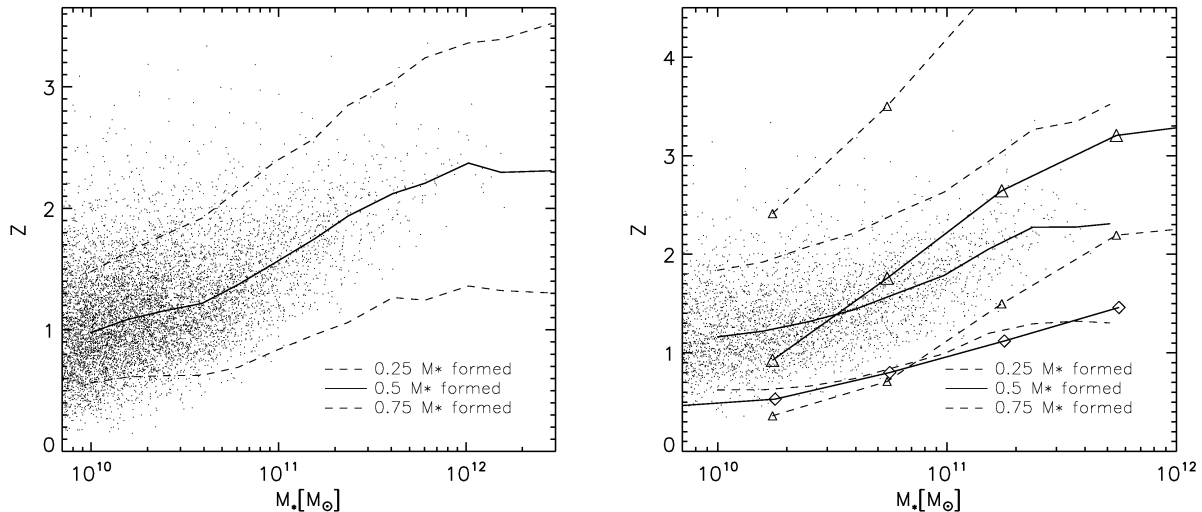


**Figure 2.** The formation redshift of the stellar component, i.e. the redshift when half of the  $z = 0$  stellar mass of a galaxy was formed, as a function of galaxy stellar mass (points). The lines show the median redshift at which galaxies formed 25, 50, and 75 percent of their  $z = 0$  stellar mass. Left: formation redshifts as a function of simulated mass. Right: Simulated masses are rescaled to match the observed SMF. We compare the simulated data (lines without points), with the observationally inferred formation redshifts from Panter et al. (2007) (triangles) and Gallazzi et al. (2008) (diamonds).

but especially at the low mass end. We show the formation redshift of 50 percent of the galaxy stellar component (diamonds) from their Figure 9 (they do not provide 25th and 75th percentiles). To compare the simulated galaxies to these observations we correct the simulated galaxy stellar masses by the correction factor from Figure 1. By comparing the stellar formation redshift in the simulations to the observed values, one can infer whether the bulk of such a mass correction, which in nature would happen through some feedback mechanism, needs to occur below the observationally inferred formation redshift, in the case where the observed formation redshifts are higher than those simulated or above the observational redshift in the opposite case. Both the observational results and our simulation show that stars in the progenitors of massive galaxies form very early. However, at the high mass end the simulated stellar ages are in rough agreement with the results of Panter et al. (2007) but are much higher than those of Gallazzi et al. (2008). It is beyond the scope of this paper to track the differences in the observationally inferred stellar ages, but it is clear that the systematic uncertainties in these estimates are still very significant. While the differences between the observed datasets are large at the low mass end, both observational estimates indicate that the simulated galaxies form too early, implying that their formation should be more suppressed at early times (we discuss this in more detail in § 4.1).

In Figure 3, we show the contribution of gas initially accreted through cold mode to the final masses of galaxies at  $z = 2$  and  $z = 0$  (the second panel is similar to Figure 7 in K09). The dispersion in the cold mode fractions is large at all masses, but the overall trends with galaxy mass (indicated with the median line) are clear. We demonstrated in K09 that at  $z > 2$ , cold mode accretion completely dominates the smooth gas accretion at all masses. Around  $z = 2$ , hot mode starts to be an important source of gas in

a limited mass range, around few times  $10^{10} M_\odot$ . However, from Figure 3 one can see that typical high-redshift galaxies at any mass build up 90–100 percent of their mass through cold mode accretion, making the hot mode contribution insignificant at these early times.

The situation is a bit more complicated at  $z = 0$ . As expected, a typical low mass galaxy forms almost completely through cold mode accretion. The contribution of hot mode accretion increases with mass up to a maximum of 25–30 percent for galaxies with masses of around  $\sim 4\text{--}5 \times 10^{10} M_\odot$ , but then the trend reverses and the median hot mode contribution decreases in more massive galaxies. (We emphasise that this hot mode contribution is measured over the entire history of the baryons that make up the galaxy, whereas a plot of the *current* accretion would show much larger hot mode fractions.) The increase in the cold mode contribution at higher masses owes to the increased contribution of mergers, which mostly adds material that was originally accreted through cold mode. This occurs because the merging progenitor galaxies accrete the bulk of their mass at much earlier times when cold mode accretion dominates the buildup of galaxies at all masses. This trend is reinforced by the lack of substantial hot mode accretion in massive halos at  $z < 2$ . The mass dependence of the cold mode fractions also explains why the simulated mass function is most affected by hot mode removal at masses of  $\sim 0.3\text{--}1 \times 10^{11} M_\odot$ , since these are the galaxies that had the largest fractions of their total mass accreted through hot mode.

In Figure 3 we also plot the median fraction of mass initially accreted in cold mode after the cold mode accretion is removed from massive galaxies as described in § 2.2. The residual cold drizzle contributes around 20 percent to the galaxy mass, so removing it increases the ratio of hot to cold mode by around 20 percent; since this ratio is it-



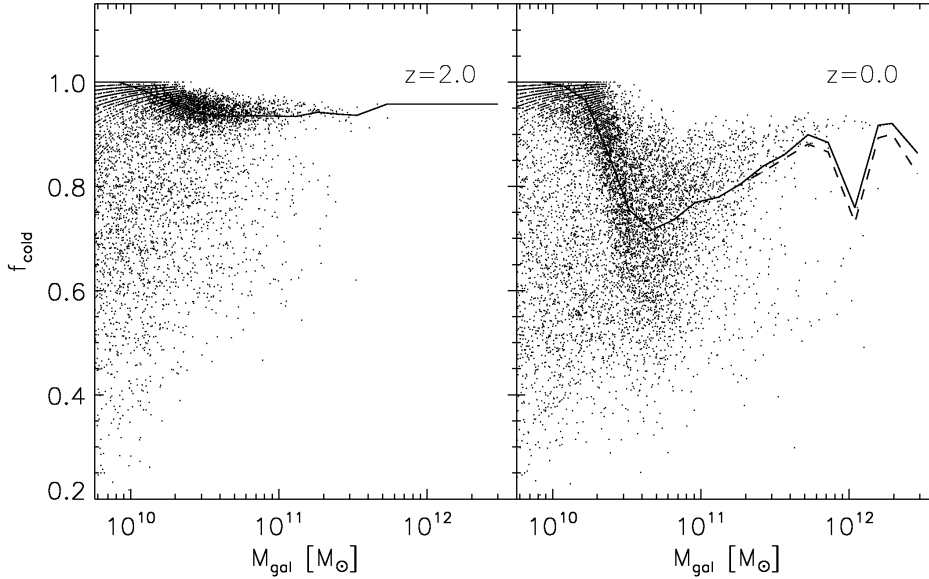


**Figure 3.** The fraction of galactic baryonic mass initially accreted through cold mode plotted as a function of galaxy mass at  $z = 2$  and  $z = 0$ . The solid line plots the median fraction acquired through cold mode, and the dashed line shows the median cold mode fraction after the removal of potentially spurious cold mode for massive galaxies (only at  $z = 0$ ), in bins of 0.15 dex in mass.

self small, this change raises the cold mode contribution by several percentage points at most.

From Figure 2, it is clear that bulk of the stellar mass in massive galaxies forms prior to  $z = 2$ , in much smaller objects whose formation is completely dominated by cold mode accretion. The most massive progenitors of these galaxies at  $z > 2$  contain typically only  $\sim 20$ – $25$  percent of their present mass. These objects later merge to form even more massive galaxies. Since in high-redshift galaxies only a small fraction of the baryonic mass is gained through the cooling of hot halo gas, the removal of hot mode accretion cannot significantly affect the masses of these galaxies. Therefore, any feedback mechanism that aims to lower the masses of the most massive galaxies must actually affect the masses of their lower-mass, high-redshift progenitors as we discuss in §4.1.

### 3.3 Specific star formation rates

The final observable we shall consider is the current star formation rate of individual galaxies, which is most usefully presented relative to its mass as the specific star formation rate (SSFR). Quite frequently galaxy colour is used as a proxy for SSFR, although of course a galaxy’s colour depends on its current star formation rate, the previous star formation history, and the amount of dust attenuation. Colour-magnitude plots incorporating observations of many thousands of galaxies have become commonplace, and the main features of these plots are by now familiar (e.g. Baldry et al. 2004): there is a red sequence of galaxies, mostly populated by massive, early types with low SSFRs, distinctly offset from a blue cloud of late type, lower mass galaxies with high SSFRs. While part of this division can be caused by dust attenuation, most of the differences

are clearly caused by varying amounts of recent star formation. However, for comparison to the simulations, a plot of  $\log(\text{SSFR})$  versus galaxy stellar mass is more useful. Obtaining this requires modelling each observed galaxy’s spectral energy distribution to obtain transformations from magnitude to mass and from colours to  $\log(\text{SSFR})$ ; the latter transformation in particular is highly non-linear.

Just such a plot of the low redshift galaxy population was recently obtained by Salim et al. (2007), using UV data from the GALEX satellite (Martin et al. 2005) combined with *ugriz* photometric data from the Sloan Digital Sky Survey (SDSS) (York et al. 2000). Their analysis builds upon and supersedes earlier optical-only work by Kauffmann et al. (2003) and Brinchmann et al. (2004). The authors consider a wide range of star formation histories for every observed galaxy and assign each a likelihood, leading to a two-dimensional probability distribution of SSFR and stellar mass for each individual galaxy (where the SSFR is averaged over the last 100 Myr). If one simply plots the mean value of this distribution for individual galaxies in the observed sample, it shows an obvious bimodality, as one can see in the left panel of Figure 4. The “blue cloud” galaxies identified in a colour-magnitude diagram now correspond to a tight star-forming sequence in the upper part of the plot, partly because scatter caused by variations in metallicity and dust have been removed by the SED fitting. The tight “red sequence” of the colour-magnitude diagram now corresponds to a low-SSFR sequence, broadened by the non-linear transformation between colour and  $\log(\text{SSFR})$ , and there is a significant bridge population between the two sequences. (The relative prominence of the low-SSFR sequence in the left panel of Figure 4 is partly an artifact: there is a lower limit of  $\text{SSFR} \sim 10^{-5} \text{ Gyr}^{-1}$  allowed in the models of SSFR history used in Salim et al. (2007) causing the mean

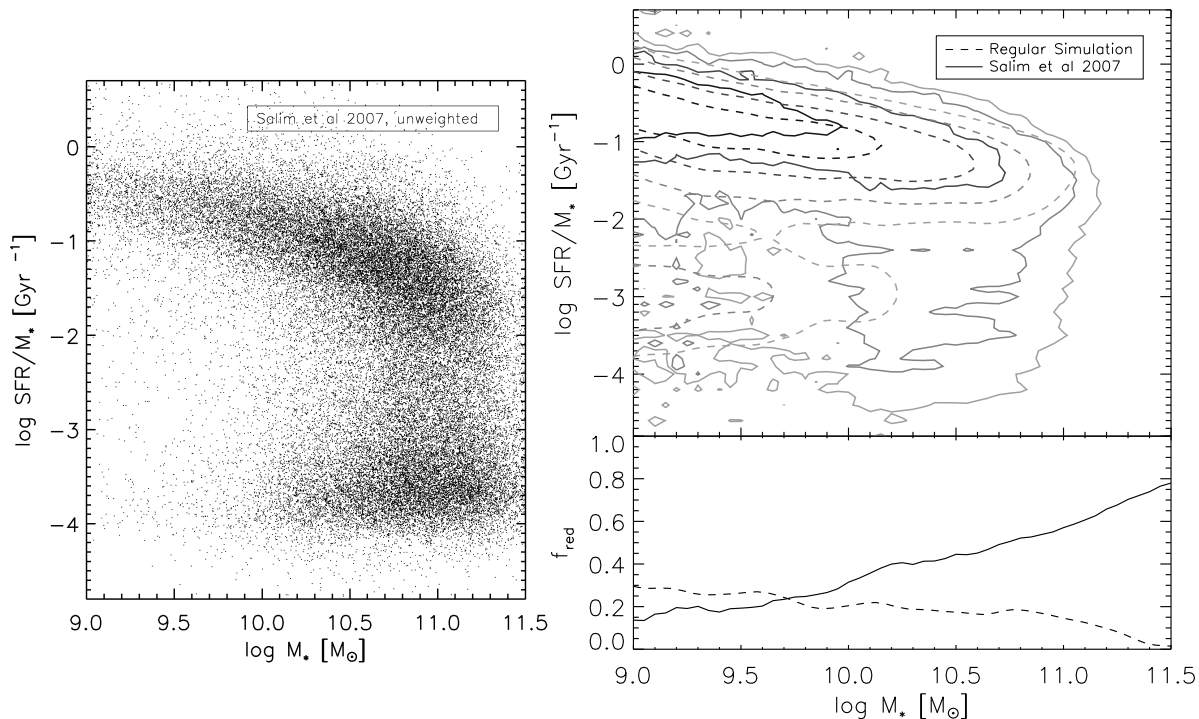


**Figure 4.** The left panel shows the distribution of individual galaxy SSFRs as a function of their stellar mass in the sample of Salim et al. (2007). Individual values represent the mean of the probability density distribution for each galaxy. The upper right panel shows contours encompassing the top 25, 50, 75 and 90 percent (from darker to lighter gray) of the observed cumulative probability density distribution in the SSFR-galaxy mass plane weighted by the effective survey volume at each mass (solid contours). The simulated galaxies are also plotted (dashed contours). The lower right panel plots the fraction of galaxies with SSFRs less than  $0.01 \text{ Gyr}^{-1}$  versus mass for the observed sample (solid line) and the simulation (dashed line). The simulated masses are re-normalised to match the observed galaxy stellar mass function (see text for details).

$\log(\text{SSFR})$  of individual low-SSFR galaxies to cluster around a value somewhat higher than this.)

A fairer representation of observed galaxies in this plot smears each individual galaxy over its full two-dimensional probability distribution in SSFRs and mass, and normalises it by the effective survey volume at each mass, i.e.  $V/V_{\text{max}}$ . We show this result, which is the only one that should be compared with simulations, as the solid contours in the right panels of Figure 4. This figure is equivalent to the grayscale image shown as the lower panel of Figure 15 in Salim et al. (2007). We generate the contours from a grid with a spacing of 0.05 in  $\log(M)$  and 0.1 in  $\log(\text{SSFR})$ , and plot contours encompassing 25, 50, 75, and 90 percent of the maximum probability density (from darkest to lightest shading).

With these changes, the lower-mass galaxies become more prominent, and the low-SSFR sequence smears out into a flat ledge covering a very wide range of SSFRs that extends downward from the star-forming sequence — in contrast to the colour-magnitude diagram, one might now describe the features as a “blue sequence” and a “red cloud”. The star-forming sequence persists as a tight SSFR vs. galaxy mass relation at relatively high SSFRs, around  $0.3 \text{ Gyr}^{-1}$  at stellar masses of  $\sim 1 - 5 \times 10^9 M_{\odot}$ . SSFRs in this sequence decrease toward higher masses. The sequence dominates the number density over several orders of magnitude in galaxy mass, up to  $\sim 10^{11} M_{\odot}$ , although some galaxies have low SSFRs even at intermediate and low galaxy masses. The tight-

ness and weak dependence on mass of this relation was discussed extensively in the literature (e.g. Noeske et al. 2007).

In the same plot, we also show the properties of the simulated galaxies. As we discussed previously, the masses of the simulated galaxies are much higher than those of observed galaxies. Hence, even if the present star formation rate in a simulated galaxy were to correspond to the observed values, the SSFRs would be much lower than those observed. To avoid this problem we correct the masses of the simulated galaxies using the correction factors  $f_{\text{corr}}$  in Figure 1, assuming that the mass rank order of the simulated galaxies is preserved. This is similar in spirit to halo and subhalo matching models that try to connect the observed properties of galaxies to the dark matter halos and sub-halos from N-body simulations (e.g. Yang et al. 2003; Vale & Ostriker 2006; Conroy et al. 2006), except in our case we are connecting observed and simulated galaxies. Furthermore, to account for the different initial mass function (IMF) used in Bell et al. (2003), a diet Salpeter (1955) IMF, and that used in Salim et al. (2007), a Kroupa (2001) IMF, we lower these corrected masses by  $\log M = 0.15$ .

We leave the SFRs of individual galaxies unchanged in this plot, so that the SSFRs increase by a factor  $f_{\text{corr}}^{-1}$ . Our reasoning is that here we are essentially examining the star formation rates as a function of halo mass, and the adjustment to the mass should just enable a fair comparison of galaxies residing in similar halos. In K09, we showed that the SFRs of individual galaxies closely follow the smooth

gas accretion rates. As we discuss in §4.1, if the mechanism that is responsible for producing the correct mass function is ejective feedback from SN-driven winds, it should not significantly affect the accretion of intergalactic gas at low redshift, when such feedback is inefficient, and hence it would also not likely affect the tight relation between gas accretion and star formation. Therefore, the long term mass accumulation of galaxies (that we are trying to correct with the mass re-normalisation) should not affect the low-redshift SFRs. Since the simulated galaxies have exact values for both their SSFRs and their masses, to compare them with the observational data we add two-dimensional Gaussian uncertainties. We choose the mass uncertainties to have  $\sigma_{\log M} = 0.07$  and the SSFR uncertainties to have  $\sigma_{\log \text{SSFR}}$  linearly decreasing from 0.6 for the lowest SSFRs to 0.2 for the highest SSFRs, both in rough agreement with the errors present in Salim et al. (2007).

Most of the simulated galaxies also reside in a well defined star forming sequence with properties that are similar to the observed star forming sequence. There is, however, a sizeable population of simulated galaxies with zero SSFR, which possibly corresponds to part of the observed red sequence. Owing to our limited mass and time resolution, the transition between zero SFR galaxies and star forming galaxies suffers from discretisation effects, with the lowest possible nonzero simulated star formation rate being around  $0.02 M_{\odot} \text{yr}^{-1}$ . When we plot these zero SSFR simulated galaxies we assign them a very low SSFR of  $\sim 10^{-3} \text{Gyr}^{-1}$ , before adding Gaussian uncertainties. While most of the observed red sequence galaxies reside at the high mass end, most of the simulated zero SSFR galaxies reside at the low mass end. Interestingly, the mass dependence and scatter of the simulated star forming sequence at  $z = 0$  is consistent with the observed trends. The median SSFRs of simulated galaxies at a given mass are very close to the observed sequence except around  $10^{10} M_{\odot}$ , where it is several tenths of a dex lower. However, as noted in §2, the current simulations do not include mass feedback from intermediate-mass stars. On average at least, this effect might boost the typical SFR by up to 0.3 dex, bringing the low-mass star-forming sequence back into agreement with the observed one, but if the same effect operates at high masses it would make their simulated SSFRs too high.

To quantify any differences in the way galaxies populate the high and low SSFR regions, approximately corresponding to “red” and “blue” galaxies, we determine the fraction of galaxies with SSFRs lower and higher than  $0.01 \text{Gyr}^{-1}$ . We plot the fraction of low SSFR galaxies in the lower-right panel of Figure 4 for both observed (solid line) and simulated (dashed line) galaxies. The observed galaxy sample has about 20 percent of its galaxies in the red sequence for  $M_{\text{gal}} < 10^{10} M_{\odot}$ . In the simulation the fraction of low SSFR galaxies is about 25–30 percent, which is slightly higher than the observed fraction. However, the differences begin to increase towards higher masses and by around  $10^{11} M_{\odot}$  about 60 percent of the observed galaxies have very low SSFRs while all but 15 percent of the simulated galaxies reside on the star forming sequence. The discrepancies get even larger at higher masses. This illustrates a generic problem that occurs for massive galaxies in simulations and SAMs without feedback: they form too many stars at late times and hence are too blue on average.

The differences between the simulated and observed galaxies in Figure 4 thus show some different symptoms than those in the mass function plot (Fig. 1). At low masses the current star formation rates agree well with the observations, whereas the simulation masses are much higher. Alternatively, whereas the masses should be reduced at high redshift by ejective feedback from SN-driven winds, perhaps it should not significantly affect the gas supply and star formation rates at low redshift when such feedback is inefficient (as we discuss in §4.1). Starting at  $\sim 10^{10} M_{\odot}$  where the simulated masses are in the best agreement, however, the fraction of star-forming galaxies starts to diverge strongly from the observed fractions, even though the actual star formation rates of those galaxies still on the star-forming sequence are in reasonable agreement.

As we did with the mass function, to mimic an extreme version of preventive feedback in hot halos, we completely remove all the hot mode accretion and plot the resulting galactic properties in the left panels of Figure 5. We again re-normalise the galaxy masses to match the observed mass function after the removal of the hot mode in the same way as in Figure 4. This hot mode removal does not change any of the properties at the low mass end because these galaxies accrete their gas almost exclusively through cold mode accretion. As we showed before, even the highest mass galaxies do not significantly change their masses when hot mode accretion is removed, but they do significantly change their SSFRs. Up to masses of  $M_{*} \sim 10^{11} M_{\odot}$ , the average SSFRs of simulated galaxies change enough to be roughly consistent with the observed galaxies. However, if one looks more closely this leaves too few galaxies to correspond to the observed star forming sequence. Even at intermediate masses of around  $10^{10} M_{\odot}$ , the removal of the hot mode ruins the relatively good agreement between the observed and simulated star forming sequence. Although the fraction of galaxies below our adopted “red sequence threshold” is similar to the observed fraction, the typical SSFR of a star forming galaxy is now factor of 3–5 lower than those observed. Even if one were to include mass feedback from intermediate-mass stars as in §2, the SSFR would still be low by a factor of about two. This suggests the need for a selective feedback mechanism, which only significantly affects star formation in a fraction of the galaxies at a given mass to preserve the star forming sequence. Finally, at masses greater than  $6 - 7 \times 10^{10} M_{\odot}$  the discrepancies persist and are as large as when the hot mode is not removed.

In the right panels of Figure 5, we remove both the hot mode accretion and the cold mode accretion in galaxies more massive than  $10^{11} M_{\odot}$  (before the mass re-normalisation), i.e. the possibly spurious cold drizzle. We again renormalise the stellar masses of galaxies using the corrections from Figure 1 to match to observed mass function. The SSFRs of the galaxies at the massive end are reduced even further and are more similar on average to the observed massive galaxies than when we only remove the hot mode accretion. The rough agreement in the red fraction now extends up to galaxy masses of about  $2 \times 10^{11} M_{\odot}$  with the more massive galaxies remaining discrepant. However, once again there are not enough galaxies on the star forming sequence owing to the nature of our mock feedback that affects approximately all galaxies above a given mass (in the case of cold drizzle removal) and above a given halo mass (in the

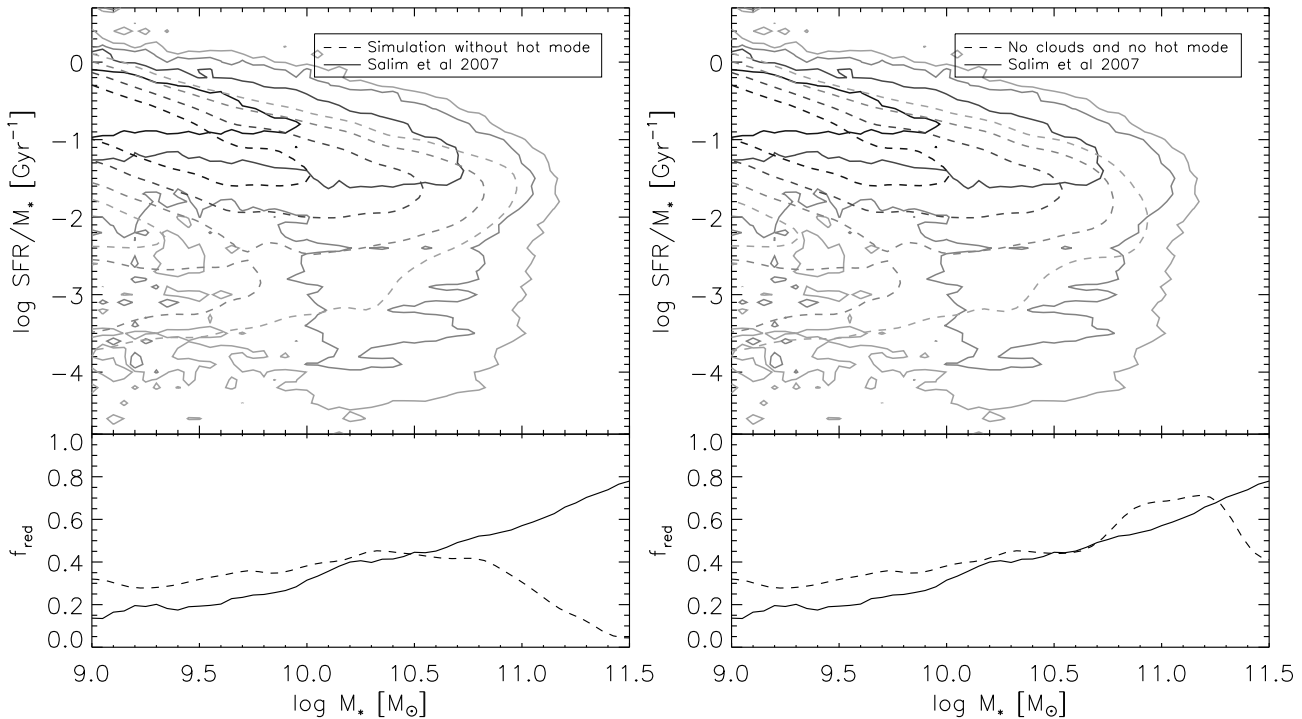


**Figure 5.** Same as the right panel of Figure 4, but the simulation results are computed after suppressing all hot mode accretion (left) or all hot mode accretion and all “cold drizzle” in massive ( $M_* > 10^{11} M_\odot$ ) galaxies (right).

case of hot mode removal). Again, the need for a more selective feedback mechanism is obvious from the observed SSFR distribution alone, as a significant fraction of galaxies even at the largest masses appear to be part of a normal star forming sequence.

To summarise, removing all the hot mode accretion and the potentially spurious cold mode accretion from massive galaxies, yields a fraction of simulated “red” galaxies that is similar to but actually slightly higher than the observed sample around  $10^{11} M_\odot$ , suggesting that this recipe removes too much late time accretion. Furthermore, this procedure moves all galaxies away from the star-forming sequence and therefore is not supported by observations. However, the problem at the very massive end (above  $2 \times 10^{11} M_\odot$ ) remains the same, where only a small fraction of the simulated galaxies have low enough SSFRs. The removal of hot mode accretion and “cold drizzle” significantly lowers their SSFRs, but they are still higher than those observed. Therefore, preventive feedback mechanisms like radio mode AGN alone are probably not sufficient to make the most massive galaxies, those with  $M_{\text{gal}} \gtrsim 2 \times 10^{11} M_\odot$ , red enough. These massive galaxies are typically the central galaxy of a group or cluster and their SSFRs remain too high because fresh gas for star formation arrives through minor mergers. Therefore, to keep the central galaxies red enough, an efficient feedback mechanism needs to lower the gas content of the satellite galaxies before they merge, or to prevent star formation from the gas that arrives with the satellites. Another possibility is that a fraction of the gas identified as coming from mergers actually comes from stripped galactic disks (similar to the “cold drizzle”) but which we cannot identify as such. Because of our limited time spacing between the simulation outputs (and possibly the numerically enhanced infall of such cold

clumps), some of the gas stripped between two outputs can end up in the central galaxy of a massive halo by the next simulation output and, therefore, be identified as coming from merger.

## 4 DISCUSSION

### 4.1 Feedback and the galaxy mass function

Many authors emphasise the overabundance of massive galaxies and their lack of red colours in simulations and SAMs (e.g. K05, Croton et al. 2006; Bower et al. 2006; Cattaneo et al. 2007) and usually blame excessive gas cooling onto central galaxies in massive halos, i.e. hot mode accretion, for this failure. However, in K09 we demonstrated that many galaxies in massive halos have almost stopped accreting gas from their hot virialised atmospheres and their masses are still a factor of  $\sim 3$  too large compared to the observations, indicating that the problem of massive galaxy formation is more complex. Most of the material currently present in the most massive galaxies was originally acquired by smaller galaxies at very early times, as shown in Figure 2, through cold mode accretion, which dominates gas accretion in all galaxies at early times. The time by which a significant fraction of a current galaxy’s mass is already accreted into its progenitors is a strong function of galaxy mass. The most massive galaxies today have their mass accreted into their progenitors, and hence most of their stars form, before  $z \sim 2$ . Such a scenario is a natural consequence of hierarchical halo and galaxy formation and this “downsizing” effect is ubiquitous in both cosmological simulations (Dave 2006) and SAMs of galaxy formation (De Lucia & Blaizot 2007). This is the reason why preventive feedback alone, e.g. AGN

activity, cannot significantly lower the masses of the most massive galaxies, contrary to the assumptions in some popular current models.

This finding also helps us to elucidate the nature of the feedback mechanism needed to fix the problems at the high mass end in the simulated galaxy mass function. Feedback in low and intermediate mass objects that form at early times, which subsequently hierarchically merge to make the massive galaxies today, must be very efficient at high redshifts to reduce their masses before they transform that mass into stars. Since these galaxies gain most of their mass through cold mode accretion, it is natural that it should be an ejective feedback mechanism like some form of galactic winds. Standard ejective feedback mechanisms have little or no effect on cold mode accretion since the gas is already cold and has a high momentum flux. However, since cold mode dominated halos do not possess a hot halo of gas, the winds are free to leave the galaxy unimpeded as long as they have enough energy. In fact, many high redshift galaxies show evidence of very strong, high velocity outflows of gas (Shapley et al. 2003). Strong feedback in high redshift galaxies could be the consequence of momentum driven winds, which could operate in starburst galaxies (Murray et al. 2005). In this model, driving galactic outflows requires a very efficient starburst with a high star formation rate per unit surface area. At redshifts  $z \geq 2$  almost all galaxies have sufficiently high star formation rates to enable this efficient feedback mechanism (see the discussion in Oppenheimer & Davé 2006). To match the observed mass function it is probably still necessary to have some preventive feedback, especially to prevent the re-accretion of the necessarily large amounts of ejected gas. Once a galaxy's halo grows massive enough, it will gain a hot halo of gas that will impede the winds, quenching the feedback. This could lead to a natural upper mass cutoff to the ejective feedback mechanism at approximately the dividing mass between hot and cold mode halos,  $\sim 2\text{--}3 \times 10^{11} M_{\odot}$  (in reality this mass could be up to factor of 3 higher in simulations with strong outflows and metal line cooling).

Another alternative is to somehow keep the high redshift galaxies gas rich, with only a small fraction of their mass converted into stars, then remove the gas during some violent process occurring during galaxy mergers. However, this requires a significantly different star formation algorithm than we use in our simulations, which does not produce such gas-rich massive galaxies. Even then, it is not clear if quasar-driven winds or some other mechanism would be sufficient to remove enough of the gas before the progenitors merge into a massive galaxy and convert the gas into stars.

The largest differences between the observed and simulated mass functions occur at stellar masses around and below  $10^{10} M_{\odot}$  (simulated mass). Obviously, the comparison of theoretical and observational stellar mass functions highlights the need for very efficient feedback at the low mass end, but it is far from clear what mechanism actually reduces the masses of these galaxies. It is possible that a mechanism similar to the starburst driven winds that operate at high redshift, which are necessary to lower the mass function at the high mass end, are also able to lower the  $z = 0$  galaxy masses at the low mass end. However, we demonstrated that most of these galaxies acquire a large fraction of their stellar mass at late times (after  $z \sim 1.5$ ) and, there-

fore, such feedback needs to be active at late times. In general, feedback from supernova-driven winds (Dekel & Silk 1986) is the most popular candidate and is often used in SAMs (Croton et al. 2006; Somerville & Primack 1999; Cole et al. 2000). Simple calculations indicate that such feedback should be effective in halos with circular velocities up to  $V_c \sim 100 \text{ km s}^{-1}$  (Dekel & Silk 1986), which is enough to significantly affect this problematic mass range. However, realistic hydrodynamic simulations show that such feedback has difficulty significantly reducing galaxy masses in galaxies with  $M_{\text{gal}} > 10^9 M_{\odot}$  (Mac Low & Ferrara 1999; Ferrara & Tolstoy 2000), unless the star formation rates are extremely high as at high redshifts (Fujita et al. 2004). In some models the winds exhibit a thresholding behaviour: for example, in the momentum driven wind models discussed above the star formation rate surface density in most spiral galaxies at late times is not high enough to drive outflows at all after  $z < 1.5$ , except in a small number of starburst galaxies (see Martin 2005; Oppenheimer & Davé 2006 and references therein). Therefore, an additional efficient feedback mechanism appears necessary at the low mass end that can affect galaxies forming at much later times. These findings place strong requirements on cosmological simulations that model galaxy formation. The smallest objects that are often poorly resolved need to be resolved in detail at all times to understand the way feedback mechanisms interact with the infalling and galactic gas.

UV background heating can affect the formation of galaxies that would form in halos with  $M_h \lesssim 0.5\text{--}1 \times 10^{11} M_{\odot}$  at  $z = 0$  but it is efficient for only much lower mass galaxies at higher redshifts (e.g. Quinn et al. 1996; Thoul & Weinberg 1996; Gnedin 2000; Hoesft et al. 2006). Other alternatives include pre-heating by gravitational pancaking. In hierarchical galaxy formation models like  $\Lambda$ CDM, at low redshifts many intermediate mass halos form in much more massive, flattened structures. In this pre-heating scenario, one assumes that the gas in these structures is shock heated to  $\sim 5 \times 10^5 \text{ K}$ , a temperature equivalent to the expected infall velocities onto these structures, thus preventing the gas from collapsing into halos of lower virial temperature (Mo et al. 2005). However, some N-body simulations suggest that this scenario does not work in practice because halos in the problematic mass range actually form in pancakes of much lower mass and, therefore, in regions with temperatures lower than previously thought (Crain et al. 2007).

The least likely possibility we consider is that a large fraction of the baryons in late forming galaxies are locked in a gaseous component. If the observed gas fraction were substantially higher than in the simulations this would lead to a very different stellar mass function for galaxies with similar total mass. However, we checked this directly and found that our simulated baryonic mass function is no more discrepant with the observed baryonic mass function from Bell et al. (2003) than with the stellar mass function. In addition, the observed mass functions of HI gas (Rosenberg & Schneider 2002; Zwaan et al. 2005) and of the molecular gas (Keres et al. 2003) show a smaller number density of objects with gas masses comparable to the stellar masses in the most problematic mass range we analyse,  $5 \times 10^9 M_{\odot} \lesssim M \lesssim 5 \times 10^{10} M_{\odot}$ , suggesting that stellar mass dominates a galaxy's baryonic mass in this mass range. Only at lower masses does the gas begin to dominate the bary-

onic mass of galaxies (e.g. Geha et al. 2006) and hence begin to alleviate the differences between the observed and simulated stellar mass functions. However, even if the baryons in these lower mass objects remained mostly gaseous, they would greatly overproduce the observed HI mass function (Mo et al. 2005).

While the need for an ejective feedback mechanism is clear, the effect of such ejecta on the subsequent gas accretion are unknown at the present. Depending on the halo mass, wind energy, structure, metallicity and ability to diffuse metals, ejected material can have both "positive" and "negative" feedback: i.e. while it removes the gas from galaxies and adds the entropy to the surrounding gas (Davé et al. 2008) it also increases the amount of available gas in halos and pollutes halos with metals, which could increase the amount of gas that gets accreted at later times. Significant feedback at the low mass end at early times could raise the gas fractions in massive halos at later times because a smaller amount of the halo gas will be locked up in galaxies, making this effect an *intergalactic fountain*. Some fraction of the mass that is ejected from low mass galaxies could be reaccreted by higher mass galaxies at later times when such feedback might be less efficient (e.g. Oppenheimer & Davé 2008). This could lead to higher halo gas fractions, which in turn could supply more gas, thus leading to higher star formation rates in higher mass galaxies. This would increase the need for efficient preventive feedback in massive halos to remove this added late time accretion. In this sense, both ejective feedback (e.g. supernova driven winds) and preventive feedback (e.g. AGN radio mode) might be needed to yield correct galaxy masses in massive halos. However, in K09 we showed that a large fraction of massive halos naturally develop a gas density core, which might persist even in the case of higher halo gas fractions, possibly alleviating the need for additional feedback.

#### 4.2 Transforming the star forming sequence into a "red sequence"

In the previous section we showed that the observed and simulated star forming sequence of galaxies share similar properties. However, the simulations are missing a large fraction of the passively evolving galaxies with very low star formation rates, which dominate the massive end in the observations. Removing all the hot mode accretion and the (potentially spurious) cold drizzle produces a larger population of passive galaxies, but it makes the fraction of star-forming galaxies too low, especially at intermediate masses. Reproducing the observations requires a mechanism that suppresses accretion in a *fraction* of galaxies but not in all galaxies, with the fraction itself increasing from intermediate to high masses. In addition, observed red sequence galaxies are preferentially early type (morphologically) relative to galaxies on the star forming sequence (e.g. Schiminovich et al. 2007) and suppressing accretion will not in itself change a galaxy's morphology, though it can help preserve early types by preventing the regrowth of disks.

A promising candidate mechanism for moving galaxies to the red sequence is quasar and starburst driven winds, occurring during the mergers of gas rich galaxies (Di Matteo et al. 2005; Springel et al. 2005). Using the halo occupation distribution and the evolution of a type-

separated galaxy mass function, Hopkins et al. (2008, a,b) show that such a model, which assumes that star formation stops after the major mergers of gas rich galaxies, can explain the buildup of the red sequence over time as well as the fraction of red galaxies as a function of galaxy mass. The transformation from the blue to the red sequence during these events is aided by several processes: the development of a shocked hot virialised medium that slows the cooling of gas, quasar mode AGN feedback from the growing black holes, and starburst driven winds, which all occur nearly simultaneously. The fraction of galaxies at a given mass that has undergone such a transition is an increasing fraction with increasing galaxy mass, a trend that is required to be consistent with the observations. This model requires that most galaxies do not return to a star forming phase after the star formation initially stops, so a long term preventive feedback mechanism is still necessary to prevent further gas accretion, perhaps "radio mode" AGN feedback (Ciotti & Ostriker 2001; Sijacki & Springel 2006). Even the need for this "maintenance" feedback could be avoided in a large fraction of massive halos owing to the natural development of constant density cores that prevent cooling from the hot atmosphere, as we found in K09. However, if the accretion of cold gaseous clumps also occurs in massive halos (i.e. if "cold drizzle" is not a numerical artifact), then this maintenance feedback must also be able to prevent the bulk of this form of accretion. In addition, accounting for metal cooling can enhance the cooling in massive halos where it can dominate at temperatures typical of halo gas. This could make the problem of preventing the accretion and re-accretion of gas in massive halos even more severe.

Of course the major mergers of late type galaxies have the additional advantage that they result in remnants with early type morphologies (Toomre 1977; Di Matteo et al. 2005), as required for the majority of galaxies on the red sequence. Therefore, most red sequence galaxies in such models would undergo colour and morphological transformations as a consequence of the same astrophysical process. In addition, this violent feedback combination could contribute to a faster termination of the cold accretion mode in massive halos, especially at low redshift. At high redshift this might happen only in very massive halos hosting massive galaxies with modest gas fractions, because the high gas fraction of lower mass galaxies make merger driven central gas flows and therefore starburst and quasar winds less efficient (Hopkins et al. 2009).

In conclusion, AGN radio mode feedback in very massive objects, mimicked by hot mode removal, can dramatically lower the SSFRs of massive galaxies but it should not affect every object with hot mode accretion and it should have a galaxy mass dependence. The total removal of hot mode accretion removes too much recent star formation. As a consequence, semi-analytic models that completely remove this accretion in massive halos must adopt a hot mode suppression threshold mass, i.e. the mass above which hot mode is suppressed, that is higher than the mass where hot virialised halos dominate (Cattaneo et al. 2006). However, this approach, without additional assumptions, might have difficulty matching the evolution of the red sequence over time, as shown by Hopkins et al. (2008, b).

## 5 CONCLUSIONS

We describe some observational consequences of a cosmological SPH simulation of galaxy formation in a  $\Lambda$ CDM universe using Gadget-2. The simulation covers a wide dynamic range: it is able to resolve galaxies with masses larger than  $\sim 5 \times 10^9 M_\odot$  and contains several cluster size halos with masses  $> 10^{14} M_\odot$ . The SPH algorithm used in Gadget-2 is not prone to numerical overcooling. However, the simulation does not incorporate strong feedback, and, like other simulations and analytic models with weak feedback, it predicts an excessive fraction of baryons in galaxies. Detailed analysis of the simulation (see K09) allows us to understand the physics of galaxy assembly in the absence of strong feedback, and the comparison to observations in this paper indicates what form of feedback (ejective or preventive, dependence on redshift and galaxy mass) are needed to reconcile  $\Lambda$ CDM predictions with observed galaxy populations.

We compare the observed galaxy mass function with the simulation results and conclude that the simulations overproduce galaxies at all masses. The problem is most severe at the low and high mass ends. The removal of baryons that were accreted through hot mode, to mimic an extreme form of preventive feedback, only mildly lowers their mass, since the hot mode contribution to the total baryonic mass in galaxies is modest. This form of feedback is not enough to bring the stellar mass function of the simulated galaxies into agreement with the observations, even at the high mass end. This failure owes to cosmic “downsizing”, where most of the massive galaxies have already formed most of their stellar mass in smaller objects at high redshift, and these smaller systems accreted their mass through cold mode accretion.

These findings suggest that an extremely efficient feedback mechanism is necessary in high redshift galaxies at low and intermediate masses to reduce their masses substantially. Then, owing to the hierarchical nature of massive galaxy buildup, this will significantly lower the masses of these massive galaxies at late times. A natural candidate for this feedback mechanism is starburst driven winds, although our analysis does not directly constrain the exact nature of the feedback. However, since cold mode dominated galaxies must predominantly be affected, it must be some form of ejective feedback. Once the galaxy halo gains enough in mass to become hot mode accretion dominated and develops a hot atmosphere, this ejective feedback will be naturally quenched. At low redshifts an additional feedback mechanism is necessary to reduce the masses of low mass galaxies. This feedback mechanism must have the property that it substantially reduces the galaxy masses but retains similar SFRs in low and intermediate mass star forming galaxies today.

We demonstrate that most of the simulated galaxies are part of the star forming sequence whose properties are similar to the observed star forming sequence. However, while this sequence contains only a small fraction of observed galaxies at high masses, we show that a large fraction of simulated massive galaxies are still part of this star forming sequence at  $z = 0$ . Therefore, these massive galaxies have specific star formation rates that are too high on average, caused by a small amount of residual hot mode accretion, by potentially numerically induced and hence potentially spurious cold mode accretion, and by merging with gas rich

smaller objects in massive halos. The removal of the hot mode accretion, which mimics extreme preventive feedback in hot halos, like an extreme form of radio mode AGN, is enough to make the massive galaxies red enough on average. Such extreme feedback, however, should be selective since the removal of all the hot mode accretion from all galaxies ruins the agreement with the observed star forming sequence. This suggests that the feedback in halos with  $M_h > 10^{12} M_\odot$  should affect around half of galaxies with intermediate masses, e.g Milky Way mass halos, but should affect most of the galaxies in group and cluster size halos. This could be accomplished through feedback that occurs during the gas rich major mergers of galaxies, especially if such mergers occur in hot virialised halos.

We are grateful to Samir Salim for sharing with us stellar masses and SSFRs from his paper and for useful comments. D.K acknowledges the support of the ITC fellowship at the Harvard College Observatory. We also acknowledge support from NSF grant AST-0205969 and from NASA grants NAGS-13308 and NNG04GK68G.

## REFERENCES

- Agertz O., Moore B., Stadel J., Potter D., Miniati F., Read J., Mayer L., Gawryszczak A., Kravtsov A., Nordlund Å., Pearce F., Quilis V., Rudd D., Springel V., Stone J., Tasker E., Teyssier R., Wadsley J., Walder R., 2007, *MNRAS*, 380, 963
- Baldry I. K., Glazebrook K., Brinkmann J., Ivezić Ž., Lupton R. H., Nichol R. C., Szalay A. S., 2004, *ApJ*, 600, 681
- Barnes J., Hut P., 1986, *Nature*, 324, 446
- Bell E. F., de Jong R. S., 2001, *ApJ*, 550, 212
- Bell E. F., McIntosh D. H., Katz N., Weinberg M. D., 2003, *ApJS*, 149, 289
- Birboim Y., Dekel A., 2003, *MNRAS*, 345, 349
- Bower R. G., Benson A. J., Malbon R., Helly J. C., Frenk C. S., Baugh C. M., Cole S., Lacey C. G., 2006, *MNRAS*, 370, 645
- Brinchmann J., Charlot S., White S. D. M., Tremonti C., Kauffmann G., Heckman T., Brinkmann J., 2004, *MNRAS*, 351, 1151
- Cattaneo A., Blaizot J., Weinberg D. H., Kereš D., Colombi S., Davé R., Devriendt J., Guiderdoni B., Katz N., 2007, *MNRAS*, 377, 63
- Cattaneo A., Dekel A., Devriendt J., Guiderdoni B., Blaizot J., 2006, *MNRAS*, 370, 1651
- Ciotti L., Ostriker J. P., 2001, *ApJ*, 551, 131
- Cole S., Lacey C. G., Baugh C. M., Frenk C. S., 2000, *MNRAS*, 319, 168
- Conroy C., Wechsler R. H., Kravtsov A. V., 2006, *ApJ*, 647, 201
- Crain R. A., Eke V. R., Frenk C. S., Jenkins A., McCarthy I. G., Navarro J. F., Pearce F. R., 2007, *MNRAS*, 377, 41
- Croton D. J., Springel V., White S. D. M., De Lucia G., Frenk C. S., Gao L., Jenkins A., Kauffmann G., Navarro J. F., Yoshida N., 2006, *MNRAS*, 365, 11
- Dave R., 2006, in Le Brun V., Mazure A., Arnouts S., Burgarella D., eds, *The Fabulous Destiny of Galaxies: Bridging Past and Present REVIEW -Building Galaxies with Simulations*. pp 219–+

- Davé R., Oppenheimer B. D., Sivanandam S., 2008, MNRAS, 391, 110
- De Lucia G., Blaizot J., 2007, MNRAS, 375, 2
- Dekel A., Birnboim Y., 2006, MNRAS, 368, 2
- Dekel A., Silk J., 1986, ApJ, 303, 39
- Di Matteo T., Springel V., Hernquist L., 2005, Nature, 433, 604
- Ferrara A., Tolstoy E., 2000, MNRAS, 313, 291
- Fujita A., Mac Low M.-M., Ferrara A., Meiksin A., 2004, ApJ, 613, 159
- Gallazzi A., Brinchmann J., Charlot S., White S. D. M., 2008, MNRAS, 383, 1439
- Geha M., Blanton M. R., Masjedi M., West A. A., 2006, ApJ, 653, 240
- Gingold R. A., Monaghan J. J., 1977, MNRAS, 181, 375
- Gnedin N. Y., 2000, ApJ, 542, 535
- Gonzalez A. H., Zaritsky D., Zabludoff A. I., 2007, ApJ, 666, 147
- Haardt F., Madau P., 2001, in Neumann D. M., Tran J. T. V., eds, Clusters of Galaxies and the High Redshift Universe Observed in X-rays Modelling the UV/X-ray cosmic background with CUBA
- Hernquist L., 1987, ApJS, 64, 715
- Hockney R. W., Eastwood J. W., 1981, Computer Simulation Using Particles. Computer Simulation Using Particles, New York: McGraw-Hill, 1981
- Hoefl M., Yepes G., Gottlöber S., Springel V., 2006, MNRAS, 371, 401
- Hopkins P. F., Cox T. J., Kereš D., Hernquist L., 2008, ApJS, 175, 390
- Hopkins P. F., Cox T. J., Younger J. D., Hernquist L., 2009, ApJ, 691, 1168
- Hopkins P. F., Hernquist L., Cox T. J., Kereš D., 2008, ApJS, 175, 356
- Katz N., 1992, ApJ, 391, 502
- Katz N., Keres D., Dave R., Weinberg D. H., 2003, in Rosenberg J. L., Putman M. E., eds, ASSL Vol. 281: The IGM/Galaxy Connection. The Distribution of Baryons at  $z=0$  How Do Galaxies Get Their Gas?. pp 185–+
- Katz N., Weinberg D. H., Hernquist L., 1996, ApJS, 105, 19
- Kauffmann G., Heckman T. M., White S. D. M., Charlot S., Tremonti C., Peng E. W., Seibert M., Brinkmann J., Nichol R. C., SubbaRao M., York D., 2003, MNRAS, 341, 54
- Kennicutt Jr. R. C., 1998, ApJ, 498, 541
- Keres D., 2007, PhD thesis, University of Massachusetts Amherst
- Keres D., Yun M. S., Young J. S., 2003, ApJ, 582, 659
- Kereš D., Katz N., Fardal M., Davé R., Weinberg D. H., 2009, MNRAS, pp 375–+, arXiv:0809.1430 [astro-ph]
- Kereš D., Katz N., Weinberg D. H., Davé R., 2005, MNRAS, 363, 2
- Kroupa P., 2001, MNRAS, 322, 231
- Lucy L. B., 1977, AJ, 82, 1013
- Mac Low M.-M., Ferrara A., 1999, ApJ, 513, 142
- Martin C. L., 2005, ApJ, 621, 227
- Martin D. C., et al., 2005, ApJL, 619, L1
- McKee C. F., Ostriker J. P., 1977, ApJ, 218, 148
- Mo H. J., Yang X., van den Bosch F. C., Katz N., 2005, MNRAS, 363, 1155
- Murray N., Quataert E., Thompson T. A., 2005, ApJ, 618, 569
- Neistein E., van den Bosch F. C., Dekel A., 2006, MNRAS, 372, 933
- Noeske K. G., et al., 2007, ApJL, 660, L43
- Ocvirk P., Pichon C., Teyssier R., 2008, MNRAS, 390, 1326
- Oppenheimer B. D., Davé R., 2006, MNRAS, 373, 1265
- Oppenheimer B. D., Davé R., 2008, MNRAS, 387, 577
- Panter B., Jimenez R., Heavens A. F., Charlot S., 2007, MNRAS, 378, 1550
- Pearce F. R., Jenkins A., Frenk C. S., White S. D. M., Thomas P. A., Couchman H. M. P., Peacock J. A., Efstathiou G., 2001, MNRAS, 326, 649
- Quinn T., Katz N., Efstathiou G., 1996, MNRAS, 278, L49
- Rees M. J., Ostriker J. P., 1977, MNRAS, 179, 541
- Rosenberg J. L., Schneider S. E., 2002, ApJ, 567, 247
- Salim S., et al., 2007, ApJS, 173, 267
- Salpeter E. E., 1955, ApJ, 121, 161
- Schiminovich D., et al., 2007, ApJS, 173, 315
- Schmidt M., 1959, ApJ, 129, 243
- Shapley A. E., Steidel C. C., Pettini M., Adelberger K. L., 2003, ApJ, 588, 65
- Sijacki D., Springel V., 2006, MNRAS, 366, 397
- Skrutskie M. F., Cutri R. M., Stiening R., Weinberg M. D., Schneider S., Carpenter J. M., et al., 2006, AJ, 131, 1163
- Somerville R. S., Hopkins P. F., Cox T. J., Robertson B. E., Hernquist L., 2008, MNRAS, 391, 481
- Somerville R. S., Primack J. R., 1999, MNRAS, 310, 1087
- Spergel D. N., et al., 2007, ApJS, 170, 377
- Springel V., 2005, MNRAS, 364, 1105
- Springel V., Di Matteo T., Hernquist L., 2005, MNRAS, 361, 776
- Springel V., Hernquist L., 2002, MNRAS, 333, 649
- Springel V., Hernquist L., 2003, MNRAS, 339, 289
- Thoul A. A., Weinberg D. H., 1996, ApJ, 465, 608
- Tittley E. R., Pearce F. R., Couchman H. M. P., 2001, ApJ, 561, 69
- Toomre A., 1977, in Tinsley B. M., Larson R. B., eds, Evolution of Galaxies and Stellar Populations Mergers and Some Consequences. pp 401–+
- Vale A., Ostriker J. P., 2006, MNRAS, 371, 1173
- Weinberg D. H., Hernquist L., Katz N., 1997, ApJ, 477, 8
- White S. D. M., Frenk C. S., 1991, ApJ, 379, 52
- White S. D. M., Rees M. J., 1978, MNRAS, 183, 341
- Yang X., Mo H. J., van den Bosch F. C., 2003, MNRAS, 339, 1057
- York D. G., et al., 2000, AJ, 120, 1579
- Zwaan M. A., Meyer M. J., Staveley-Smith L., Webster R. L., 2005, MNRAS, 359, L30